# Thermal Efficiency and Exergy Analysis of a Solar Collector by using Roughened Absorber Plate

Shashikant Nagpure
(Research Scholar)
Mechanical Engg. Department
MANIT ,Bhopal, MP, India

Dr. K. R .Aharwal
(Associate professor)
Mechanical Engg. Department
MANI T , Bhopal, MP, India.

Dr. J .L .Bhagoria
(Professor)
Mechanical Engg. Department
MANIT , Bhopal, MP, India.

***Abstract*— The best method to save energy in a solar collector is to increase its heat transfer coefficient thereby increase the efficiency .Thermal efficiency of solar collector is lower due to low heat transfer coefficient between the absorber plate and air thereby increase plate temperature and losses to ambient. Further pumping power required may reduce benefit from solar heat. Second law of thermodynamics analysis combined with standard design procedure in a thermal system gives details of system operation also exergy analysis takes into account quality of energy transfer. Exergy analysis reveals thermodynamic faults of the thermal and chemical process. By maximizing net exergy flow sums of exergy losses including exergy loss by absorber plate temperature level is minimized and reasonably optimize design of absorber and flow ducts are getable. The present study involved developing of correlations and exergy analysis of artificial roughened solar collector and dimensionless exergy loss. The range of parameter has been decided on the basis of practical consideration and operating conditions. Experimentation has been performed on outdoor setup investigation has covered a Reynolds Number(Re) range of 2300-15000 , aspect ratio W/H is 8, relative roughness height ($e/D_h$)=0.66mm to 1.63 mm, relative roughness pitch =10,hydraulic diameter 44.44 mm, angle of attack is 60 °has been used. Result has been compared with smooth plate under similar condition to determine enhancement in exergy and dimensionless exergy loss.**

***Keywords*— *Solar air heater, Friction Factor, Pitch and Reynolds Number , Exergy , Thermal efficiency*.**

## I. INTRODUCTION

The solar air heater has an important place among solar heat collectors. It can be used as sub-systems in many systems meant for the utilization of solar energy. Possible applications of solar air heaters are drying or curing of agricultural products, space heating for comfort regeneration of dehumidifying agents, seasoning of timber, curing of industrial products such as plastics. When air at high temperature is required the design of a heater becomes complicated and very costly. As far as the ultimate application for heating air to maintain a comfortable environment is concerned, the solar air heater is the most logical choice. In general solar heaters are quite suitable for low and moderate temperatures application as their design is simple technique.

It has been found that the main thermal resistance to the convective heat transfer is due to the formation of boundary layer on the heat transferring surface. Efforts for increasing heat transfer have been directed towards artificial roughness on a surface is an effective technique to enhance heat transfer to fluid flowing in the duct by Bhagoria JLet al.[1].Artificial roughness in the form of wires and in various arrangement has been used to create turbulence near the wall or to break the boundary layer.

Thus the artificial roughness can be employed for the enhancement of heat transfer coefficient between the absorber plate and air, improving the thermal performance of solar air heater contrary to this, the excessive disturbance to the boundary layer creates more friction resulting in more pumping power by Bhagoria JLet al [2] .Application of artificial roughness in solar air heater owes its origin to several investigations carried out for enhancement of cooling of turbine blades passage. Several investigations have been carried out to study effect of artificial roughness on heat transfer and friction factor for two opposite roughened surfaces by Han[3,4],Han et al.[5-7],Wrieght et al.[8],Lue et al,[9-11],Taslim et al. and Hwang[14],Han and Park[15],Park et al.[16] developed by different investigators. The orthogonal ribs i.e. ribs arranged normal to the flow were first used in solar air heater and resulted in better heat transfer in comparison to that in conventional solar air heater by Prasad k, Mullick S.C. et al [17].Many investigators Gao x sunden B[18],Han J.C,Glicksman LR,Rohsenow WM[19],Prasad BN,Saini JS{20],Taslim ME,Li T,Kercher Dm[21],Webb RL,Eckert Erg,Goldstein RJ[22] have reported in detail the Nu and f for orthogonal and inclined rib-roughened ducts. The concept of V-shaped ribs evolved from the fact that the inclined ribs produce longitudinal vortex and hence higher heat transfer. In principal, high heat transfer coefficient region can be increased two folds with V-shape ribs and hence result in even higher heat transfer et al. [21].The beneficial effect on Nu and f caused by V-shaping of ribs in comparison to angled ribs has been experimentally endorsed by several investigators Geo X,Sunden B{23],Karwa R.[24],Kukreja RT,Lue SC, McMillin RD[25],Lau SC,McMillin RD, Han JC[26], for different roughness parameters and duct aspect ratios. For V-shape ribs, the inter-rib local heat transfer coefficient reduces from leading edge(s) to trailing edge(s) in transverse direction[21,23,24],However in the flow direction, the inter-rib local heat transfer coefficient varies like saw tooth [21,23,24].In addition, multiple V-ribs have also been investigated with the anticipation that the more number of secondary flow cells may result in still higher heat transfer et

at Lanjewar A,Bhagoria JL,Sarviya RM[27],Hans VS,Saini RP,Saini JS[28]. The second law of thermodynamic analysis

NOMENCLATURE

| | |
|---|---|
| $A_p$ | Absorber plate area, $m^2$ |
| $A_{duct}$ | Flow Cross-section area=WH, $m^2$ |
| $A_o$ | Throat area of orifice plate, $m^2$ |
| $A_s$ | Area of smooth plate, $m^2$ |
| e | Rib height ,mm |
| e/Dh | Relative roughness height |
| f | Friction factor |
| W | Duct width, m |
| H | Duct depth, m |
| K | Thermal conductivity of air, W/mK |
| m | Mass flow rate, kg/s |
| $C_d$ | Coefficient of discharge (0.62) |
| $C_p$ | Specific heat of air, KJ/kg K |
| $D_o$ | Dia of the orifice of the orifice plate |
| $D_p$ | Inside diameter of the pipe |
| H | Convective heat transfer coefficient, $W/m^2\ ^oC$ |
| Δh | Difference of height on manometer fluid |
| I | heat flux .$W/m^2$ |
| Nu | Nusselt number |
| Re | Reynolds number |
| P | Rib pitch, m |
| P/e | Relative roughness pitch |
| $T_i$ | Inlet air temperature, °C |
| $T_o$ | Outlet air temperature, °C |
| $T_{pav}$ | Mean plate temperature, °C |
| $T_{fav}$ | Average temperature of air, °C |
| V | Velocity of air |
| W/H | Channel aspect ratio |
| ΔPo | Pressure drop in duct, Pa |

combined with a standard design procedure of a thermal system gives us invaluable insight into the operation of the system. However exergy analysis, derived from both the first and second laws of thermodynamics, as compared to energy analysis, takes into account the quality of the energy transferred. The main purpose of the exergy analysis is to determine the reasons of the thermodynamic faults of the thermal and chemical processes. Exergy (or availability) analysis is powerful tool in the design, optimization, and performance evaluation of energy systems. This analysis can be used to identify the main sources of irreversibility (exergy loss) and to minimize the generation of entropy in a given process where the transfer of energy and material take place [29,30]. According to Dincer and Rosen [31], exergy analysis is an effective thermodynamic scheme for using the conservation of mass and energy principles together with the second law of thermodynamics for the design and analysis of thermal systems, and is an efficient technique for revealing whether or not and by how much it is possible to design more efficient thermal systems by reducing the inefficiencies. The concepts and definitions of exergy analysis are well recognized [32–35].

The studies of Han et al.[5],Lau et al.[10] and Taslim et al.[12] not covered the wide range of roughness and operating parameters as would be required for detailed analysis for detailed optimal design or selection of roughness parameter to be used in conventional solar air heaters. Most of the investigations carried out so far have applied artificial roughness on two opposite wall with all four walls being heated. However in case of solar air heater, roughness elements are applied to heated wall while remaining three walls are insulated. Heated wall consists of absorber plate and is subjected to uniform heat flux (insolation).This makes fluid flow and heat transfer characteristics distinctly different from those found in case of two roughened wall and four heated wall duct. Hence the present investigation has been taken up with objective of experimentation on W-shaped ribs as artificial roughness attached to underside of one broad wall of duct, to collect the data on heat transfer ,fluid flow and exergy analysis .The range of parameters covered are Reynolds number ranging from 2300-15000,aspect ratio W/H is 8,relative roughness pitch is 10,hydraulic diameter 44.44mm.

## II. EXPERIMENTAL SET UP

The experimental setup is an open flow loop that consists of a test duct with entrance & exit section, a blower, control valve, orifice plate and various devices for measurement of temperature & fluid head.

A schematic diagram of outdoor experimental setup including test section is shown in figure no.1

The flow system consists of an entry section, a test section, an exit section, a flow meter and a centrifugal blower. The set-up consists of two identical wooden ducts. Each duct is of size 2030 mm x 200 mm x 25 mm (dimensions of inner cross section) and is constructed from wooden panels of 32 mm thickness. The test section is of length 1500 mm .The test section of one of the duct carries the roughened absorber plate at the top, while the other duct carries a smooth absorber plates. The sun facing side of absorber plates are smooth and coated with blackboard paint.

A short entrance length is chosen because for a roughened duct the thermally fully developed flow is established in a short length ≈4D .For the turbulent flow regime, ASHRAE standard 93-77 recommends entry and exit length of 2.5√WH and 5√WH, respectively. The exit section of 353 mm length is used after 100 mm, three equally spaced baffles are provided in 100 mm length.

For the purpose of mixing the hot air coming out of the entire set-up, from the inlet to orifice plate, is insulated with 25 mm thick thermocol. The heated plate is 1 mm thick aluminum plate with different rib thickness roughness formed on its rear side and this forms the top broad wall of the duct, while the bottom wall is formed by 32 mm wood with insulation below it. The top sides of the entry and exit sections of the duct are covered with smooth faced 12mm thick plywood. The mass flow rate of air is measured by means of an orifice meter connected with an inclined

manometer, and the flow is controlled by the control valve provided in the lines .The orifice plate has been designed for the flow measurement in the pipe of inner diameter of 53 mm. The orifice plate is fitted between the circular G.I. pipe provided was based on pipe diameter $d_1$ which is minimum of $5d_1$ on the upstream side and $10d_1$ on the downstream side of the orifice plate In the present experimental setup we used 900 mm ($17d_1$) pipe length on the upstream side and 600 mm ($11.3d_1$) on the downstream side .The calibrated copper constantan 0.3 mm (24 SWG) thermocouples were used to measure the air and the heated plate temperatures at different locations. A digital voltmeter is used to indicate the output of thermocouples. The pressure drop across the test section was measured by a micro-manometer.

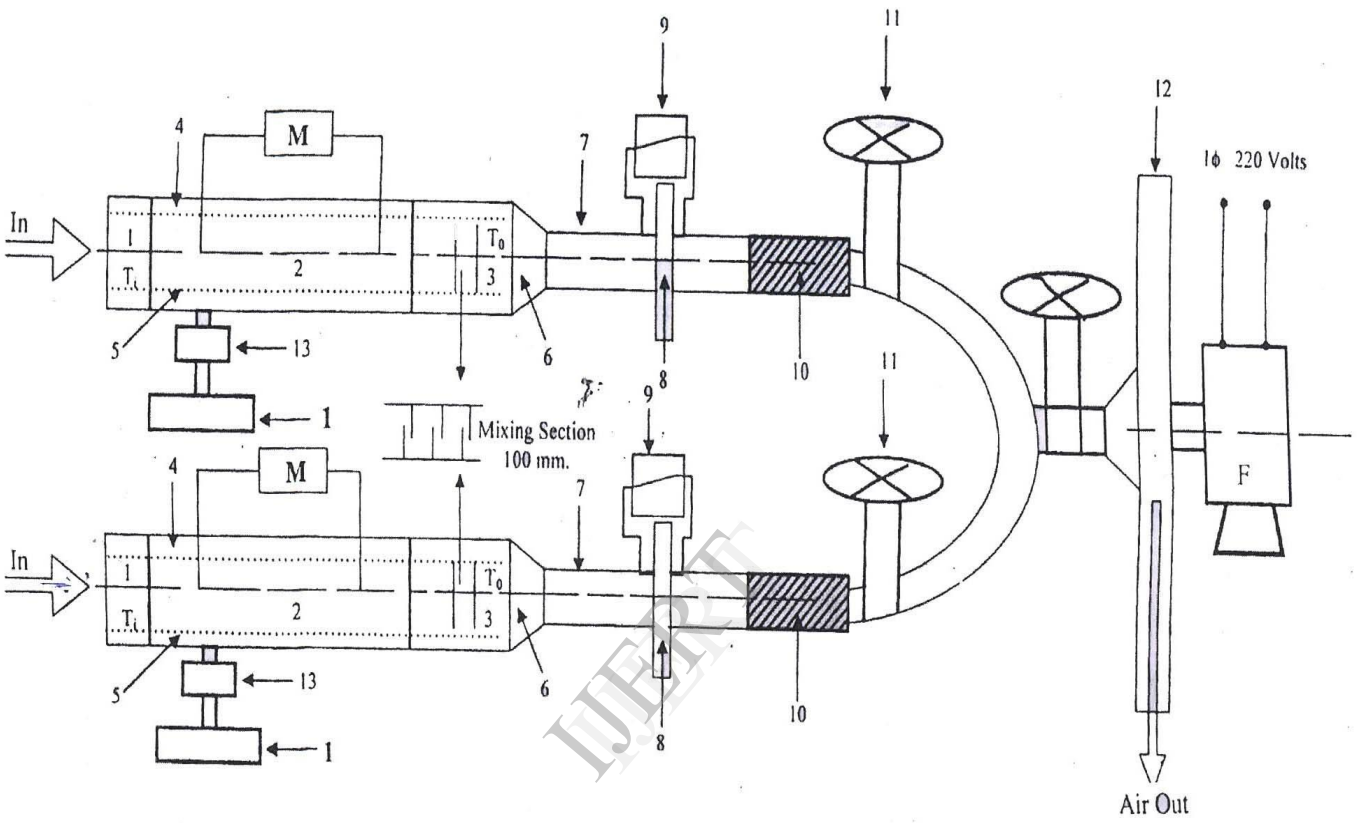


| | | | | | | |
|---|---|---|---|---|---|---|
| 1. | Entrance Length, 177 | 8. | Orifice Plate | MM | - | Micro manometer |
| 2. | Test Section, 1500 | 9. | Inclined Manometer | $T_i$ | - | Inlet Air Temperature |
| 3. | Exit Section, 353 | 10. | Flexible Pipe, 1.0 m | $T_o$ | - | Outlet Air Temperature |
| 4. | Absorber Plate, 1500 x 200 | 11. | Control Valve | | | |
| 5. | Duct Lower Side | 12. | Blower | | | |
| 6. | Transition Section | 13. | Selector Switch | | | |
| 7. | G.I. Pipe, 53mm f | 14. | Digital Micro Voltmeter | | | |

Fig No.1 Schematic Diagram of Outdoor Experimental Set-up

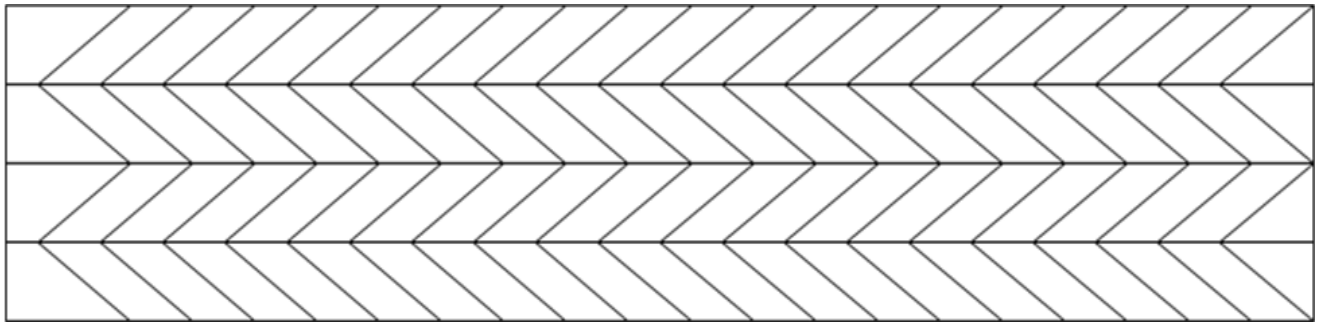

Fig.No.2 Absorber plate showing the roughness element.

A detailed description of the major components of the experimental set-up is given below:

**Roughened Duct:** The duct of rectangular cross section, consist of a wooden channel 2030 mm long and 220 mm wide which includes three sections, namely, the entrance section, test section and exit section of 177, 1500 and 353 mm length respectively. Three pairs of replacable wooden strips are used on the sides of the channel for fixing the roughened plate or covers to form of rectangular duct 200 mm wide.

A short entrance length is chosen because for a roughened duct the thermally fully developed flow is established in a short length ≈4D.For the turbulent flow regime, ASHRAE standard 93-77 recommends entry and exit length of 2.5 √WH and 5√WH, respectively. The exit section of 353 mm length is used after the test section in order to reduce the end effect in the test section. In the exit section after 100 mm three equally spaced baffles are provided in 100 mm length for the purpose

of mixing the hot air coming out of solar air duct to obtain a uniform temperature of air at the outlet.

**Roughened Plate:** Aluminium sheet (1 mm thick) 1.5 m x 0.20 m in size wall used as artificially roughened plate of the duct. The top surface of the plate was painted black with black board paint. Artificial roughness was produced on the bottom side by circular rib.

INSTRUMENTATION

The following instrumentation is used for measurement of temperatures; flow and pressure drop in duct.

**Temperature Measurement:** Calibrated copper constantan thermocouples with fiber glass insulation all along its length have been used to measure the air and plate temperature.

**Airflow Measurements:** The flow rate of air through the duct was measured by means of a pre-calibrated orifice meter. It is provided in circular pipe. An inclined tube manometer with mercury as manometric fluid and a least count of 0.1cm of mercury was used for the measurement of pressure drop across the orifice plate.

**Pressure Drop in Ducts:** A micro-manometer having a list count of 0.0025 mm was used for the measurement of pressure drop across the test section .The micro-manometer consists of a movable reservoir and an inclined transparent tube connected to the movable reservoir through flexible tubing. The reservoir is mounted on a sliding arrangement with a screw having a pitch of 20mm and a graduated dial having 400 divisions, each division showing a movement of 0.005m of the reservoir. The advantage of this type of manometer is to minimize the capillary and meniscus errors. The meniscus is maintained at fixed scribed mark by moving the reservoir up or down and movement is noted giving the pressure difference across the two pressure tapping.

**Solar Radiation Measurement:** The solar radiation intensity is measured by means of calibrated precision Pyranometer ; the output being displayed on a digital voltmeter with a least count of 0.01 mv.

## III. EXPERIMENTAL PROCEDURE

All components of the experimental setup and the instruments have been checked for proper operation. The glass covers of the collectors were cleaned before starting the experiments. The blower is then switched on and the joints of the setup are checked for air leakage with soap bubble technique.

Micro manometer and inclined U-tube manometer are properly leveled. Blower is switched on and the flow control valve is adjusted to give a predetermined rate of airflow to the test section. In order to reduce the effect of in accuracy of the calculation of the heat transfer coefficient, the temperature of the air through the duct has been maintained greater than 10 degree centigrade and the temperature difference between the heated plate and the bulk air temperature has been kept above 20 degree centigrade. During the experimentation the temperature of air entering the duct range between 38°C to 43.6°C according to the local atmospheric conditions. The temperature of the air at the outlet of the test section ranges between about 41°C to 73°C.

All readings have been noted under steady state condition which was assumed to have been obtained when the plate and air outlet temperature did not deviate over a 15 min. period. The steady state for each run has been observed to arrive in about 2 to 2.5 hours. After the steady state has reached, the heater assembly voltage and current, the plate temperatures, the inlet and exit air temperatures and the pressure drop across the duct and across the orifice plate have been recorded. For each rib configuration 15 runs have been conducted at air-flow rated corresponding to the flow Reynolds numbers between 2300 and 15000.

The following parameters were measured during the experiments:

1. Pressure drop across the orifice plate
2. Inlet air temperature of collectors
3. Outlet air temperature of collectors
4. Temperature of plate
5. Solar radiation intensity

**Data Reduction**

Steady state value of the plate and air temperatures in the duct at various locations were obtained for a given heat flux and mass flow rate of air. Heat transfer rate to the air. Nusselt number and friction factor have been computed from the data. These values have been used to investigate the effect of various influencing parameters viz. the flow rate, the relative roughness height and the angle of attack of flow on the Nusselt number and friction factor.

**Mean air and plate temperatures**

The mean air temperature or average flow temperature $T_{fav}$ is the simple arithmetic

Mean of the measure values at the inlet and exit of the test section. Thus,

$T_{f\,av} = (T_i + T_{oav})/2$

**Pressure drop calculation**

Pressure drop measurement across the orifice plate was made by using the following

$\Delta P_o = \Delta h \times 9.81 \times \rho_m \times 1/5$

Where

$\Delta P_o$= Pressure diff.
$\rho_m$= Density of the fluid
$\Delta h$= Difference of liquid head in U-tube manometer.

**Mass flow measurement**

Mass flow rate of air has been determined from pressure drop measurement across the orifice plate by using the following relationship:

$m = C_d \times A_o \times [2\rho\ \Delta P/(1 - ß^4)]^{0.5}$

where

m= Mass flow rate, Kg/s
$C_d$ = Coefficient of discharge of orifice i.e. 0.62
$A_0$= Area of orifice plate, $m^2$
$\rho_m$= Density of the air i.e 1.1576
ß =Ratio of dia.($d_o$/ $d_p$) i.e 26.5/53=0.5
ranging from 25 to 40 percent and variation was small.

**Velocity measurement**

$V = m / \rho WH$

Where
m=Mass flow rate, Kg/s
ρ=Density of air i.e. 1.1415 Kg/m3
H=Height of the duct, m (0.025)
W= Width of duct, m (0.2).

**Reynolds number**

The Reynolds number for flow of air in the duct is calculated from:

$Re = VD / \nu$,

Where,
$\nu$ = 15.48 X $10^{-6}$ $m^2$/sec, and
hydraulic diameter D = 4WH / 2(W+H)

**Heat Transfer Coefficient**

Heat transfer rate, $Q_a$, to the air is given by

$Q_a = m\, C_p\, (t_o - t_i)$

The Heat Transfer Coefficient for the heated test section has been calculated from

$H = Q_a / A_p\, (t_{pav} - t_{fav})$

$A_p$ is the heat transfer area assumed to be the corresponding smooth plate area.

**Nusselt number**

The Heat Transfer Coefficient has been used the determine the Nusselt number and Stanton number defined as:

$Nu = hD/k$

Where,

k is the thermal conductivity of the air at the mean air temperature and D is the hydraulic diameter based on entire wetted parameter.

The effect of the humidity has been neglected since the relative humidity values during the experimentation have been found to be low

**Friction Factor:**

$F = (2 * \Delta P_{micro} * D_h * \rho)/(4 * 1.3 * G^2)$

Friction factor is given by:

**Thermal efficiency:**

The efficiency is calculated By:

$\eta = Q_a / A_p I$

where,
I= Heat flux

**Exergy**

Exergy is the amount of maximum work obtained theoretically at the end of a reversible process in which equilibrium with environment should be obtained. According to this definition, in order to calculate exergy, the environment conditions should be known [6Exergy balance in a steady state open system can be written as follows

$$\sum E_i - \sum E_o + \sum E_{product} = 0 \qquad (1)$$

The Lost work as being described between differences of maximum work with real work

$$W_{lost} = W_{max} - W_{real} = E \qquad (2)$$

This expression is equal to exergy loss. Therefore, exergy loss in the open systems;

$$E = \sum m_i(h_i - T_e S_o) - \sum m_o(h_o - T_e S_o) + \sum Q\left(1 - \frac{T_e}{T_s}\right) - W \quad (3)$$

Eq. (3) gives the balance of exergy in the collector. If it is assumed that the collector has a single entrance and exit and the air is ideal fluid and also the conditions are at steady state for Eq. (3)

$$E = m(e_i - e_o) + E_R \quad (4)$$

can be written. Here,

$$e_i = (h_i - T_e S_l) - (h_e - T_e S_e) \quad (5)$$

$$e_o = (h_o - T_e S_o) - (h_e - T_e S_e) \quad (6)$$

and inserting these into Eq. (4)

$$E = m(h_i - h_o) - T_e(S_o - S_i) + I.A.(1 - T_e/T_s) \quad (7)$$

for changing of enthalpy and entropy

$$\Delta h = C_p \Delta T \quad (8)$$

$$\Delta S = C_p . In(T_o/T_i) - R.In(P_o/P_i) \quad (9)$$

If Eqs. (8) and (9) are inserted into Eq. (7)

$$E = m.C_p.\Delta T - m.C_p.T_e.In(T_o/T_i) - m.R.T_e.In(P_o/P_i) + I.A.(1 - T_e/T_s) \quad (10)$$

is obtained.

$$E = \frac{E}{Q} = \frac{T_e}{\Delta T}.In\left(\frac{(T_o/T_i)}{(P_o/P_i)^{\frac{k-1}{k}}}\right) + \frac{1}{\eta}\left(1 - \frac{T_e}{T_s}\right) - 1 \quad (11)$$

the equation of dimensionless exergy is obtained

## IV. RESULT AND DISCUSSION

Figure 1. shows the variation of Nusselt Number with Reynolds Number for different roughness .It is found that the Reynolds Number increases heat transfer increases because Nusselt Number is nothing but the ratio of conductive resistance to boundary layer decreases and hence convective resistance decreases , which in turn increases the Nusselt Number . It can be seen from this figure that the Nussult Number values increases rapidly with Reynolds Number is increases.

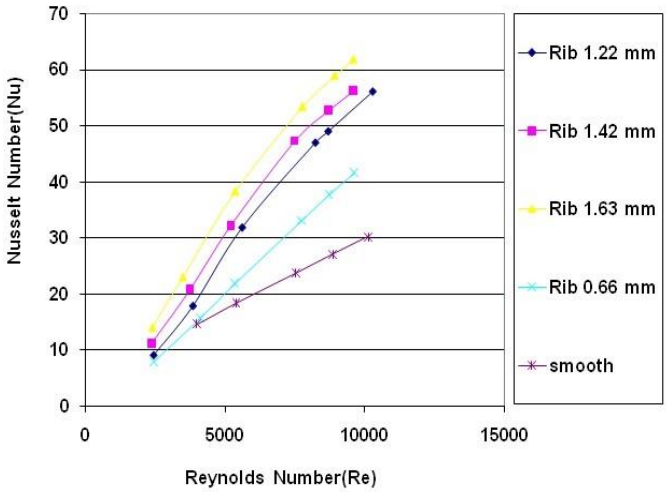


Fig: 3 Reynolds Number Vs Nusselt Number

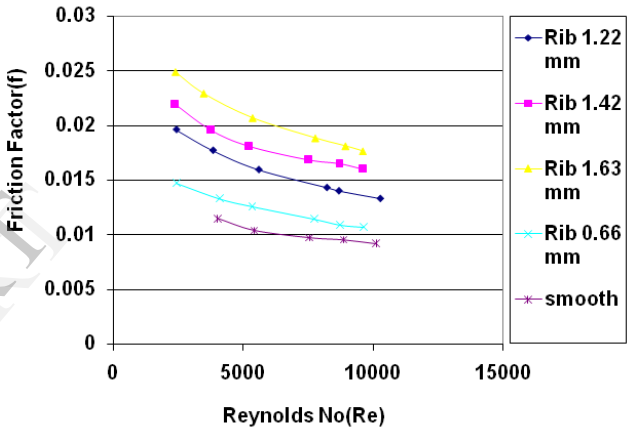


Fig:4 Reynolds Number Vs Friction Factor

Figure 3.shows the variation of Thermal efficiency with respect to Reynolds number. When Reynolds number is low the roughness elements lie within the thermal boundary layer and velocity of air is not sufficient to break the Figure 2.shows the plots of experimental values of the friction factor as the function of Reynolds number for smooth plate and rough surface with different roughness .Friction factor can be considered as the inverse of Reynolds number within the range of investigation .Thus from Figure it is cleared that value of friction factor drop proportionally as the Reynolds number increases because of the suppression of viscous sublayer.

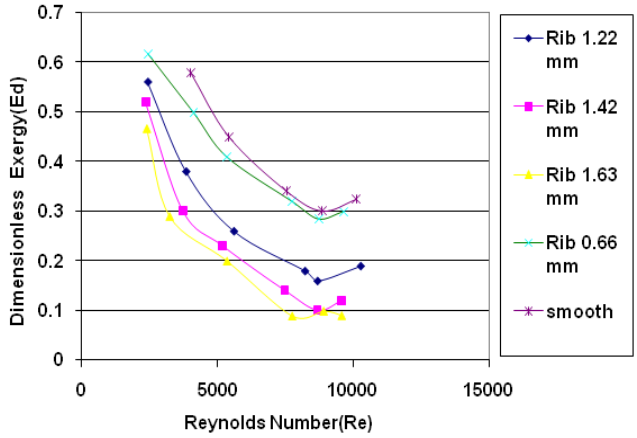


**Fig: 6 Reynolds Number Vs Dimensionless Exergy**

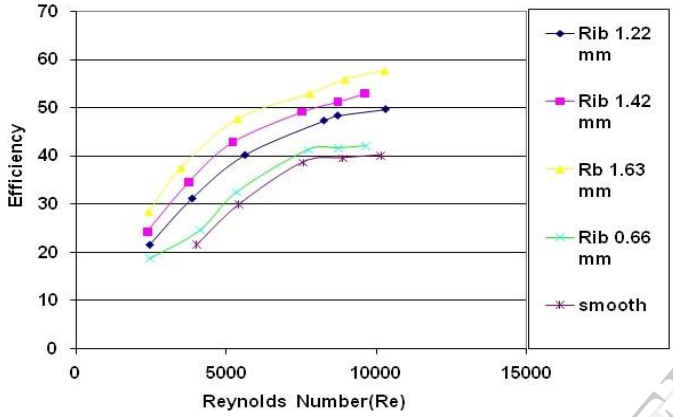


**Fig: 5 Reynolds No Vs Efficiency**

Figure 3.shows the variation of Thermal efficiency with respect to Reynolds number. When Reynolds number is low the roughness elements lie within the thermal boundary layer and velocity of air is not sufficient to break the thermal boundary layer As found by experiment that the thermal efficiency increases rapidly in lower Reynolds number region and in the region of high Reynolds number rate of increase of thermal efficiency is lower. With retard the flow rate. The experimental values of the thermal efficiency of the four roughened absorber plates tested have been compared with smooth plate. It is cleared from the figure that as compare with a conventional smooth duct solar air heater, the thermal efficiency increases at the increases Rib thickness of the absorber plate.

For air flow over a W-shape ribs separation occurs not only at the top edge of the rib but also at the edges at the end of the ribs,this secondary flow may also interrupt the growth of the boundary layer of the nearby reattachment zones.

The dimensionless exergy loss is obtained from figures 4, which increase significantly according to the result calculated for each collector. Since the exergy loss changes with ambient conditions a theoretical correlation does not exist in the literature. However, in our study it approximately can be applied for minimum exergy loss. The dimension less exergy loss is obtained from equation. The exergy loss change with ambient conditions, if the solar collectors are considered as a heat exchanger, the maximum heat transfer occurs in case of discharging the collector at the surface temperature of the air inlet and minimum heat loss occurs. According to this statement, for the maximum heat transfer the following equation can be used.

$$Q_a = m C_p (t_o - t_i)$$

As seen in figure,the lowest exergy loss occurred in rib height 1.6mm.There is a reverse relationship between dimensionless exergy loss and collector efficiency as well as temperature difference .It is clear that when the efficiency is maximum value, the exergy loss is minimum.

## CONCLUSION

On the basis of is investigation on heat transfer characteristics in solar air duct having wire mesh on absorber plate, the following conclusions have been drawn :-

1. The solar air heater gives best performance at about 12:30 pm. When solar intensity is maximum.
2. Efficiency increase with the increase in Reynolds number.
3. Dimensionless exergy decreases with increase Reynolds number
4. Thermal efficiency of roughened duct is increase as compare to smooth duct at same Reynolds Number
5. Roughened area of plate has a significant effect on the heat transfer coefficient.
6. The experimental value of the thermal efficiency of the four absorber plates tested has been compare with that smooth plate. Rough plate $e/D_h$ = 1.66 mm, gives highest efficiency.

## REFERENCES

[1] Bhagoria J.L. "Fluid Flow and Heat Transfer studies on Artificial Roughness in Solar. Air Heater Duct", Ph.D. Thesis, Dept. of Mechanical Engineering, IIT Roorkee.
[2] Bhagoria J.L., "Heat Transfer coefficient and Friction factor correlations for rectangular Solar Air Heater duct having transverse wedge shaped rib Roughness on the Absorber Plate", Int. J. of Renewable Energy, Vol. 25, 2002, 341-369.
[3] Han JC. Heat transfer and friction in channels with two opposite rib roughened walls. J Heat Transfer 1984; 106(4):774-81.
[4] Han JC. Heat transfer and friction characteristics in rectangular channels with rib turbulators. J Heat Transfer 1988;110(2):321-8.
[5] Han JC, Glicksman LR, Rohsenow WM. An investigation of heat transfer and friction for rib roughened surfaces. Int J Heat Mass Transfer 1978;21(8)1143-56.
[6] Han JC, Park JS, Lei CK. Heat transfer enhancement in channels with turbulence promoters. J Eng Gas Turbines Power 1985;107(3):628-35.
[7] Han JC, Zhang YM, Lee CP. Augmented heat transfer in square channels with parallel, crossed, and V-shaped angled ribs. J Heat Transfer 1991;113(3):590-6.
[8] Wright LM, Fu WL, Han JC. Thermal performance of angled, V-shaped, and Wshaped rib turbulators in rotating rectangular cooling channels (A=R4:1).J Turbomachinery 2004;126(4):604-14.
[9] Lau SC, Kukreja RT, Mcmillin RD. Effects of V-shaped rib arrays on turbulent heat transfer and friction of fully developed flow in a square channel. Int JHeat Mass Transfer 1991;34(7):1605-16.
[10] Lau SC, Mcmillin RD, Han JC. Turbulent heat transfer and friction in a square channel with discrete rib turbulators. J Turbomachinery 1991; 113(3):360-6.
[11] Lau SC, Mcmillin RD, Han JC. Heat transfer characteristics of turbulent flow in a square channel with angled discrete ribs. J Turbomachinery1991;113(3):367-74.
[12] Taslim ME, Bondi LA, Kercher DM.An experimental investigation of heat transfer in an orthogonally rotating channel roughened with 45 deg crisscross ribs on two opposite walls. J Turbomachinery 1991;113(3):346-53.
[13] Taslim ME, Li T, Kercher DM. Experimental heat transfer and friction in channels roughened with angled, V-shaped, and discrete ribs on two opposite walls. J Turbomachinery 1996;118(1):20-8.

[14] Liou TM, Hwang JM. Effect of ridge shapes on turbulent heat transfer and friction in a rectangular channel. Int J Heat Mass Transfer 1993;36(4):931-40.
[15] Han JC, Park JS. Developing heat transfer in rectangular channels with rib turbulators. Int J Heat Mass Transfer 1988;31(1):183-95.
[16] Park JS, Han JC, Huang Y, Ou S, Boyle RJ. Heat transfer performance comparisons of five different rectangular channels with parallel angled ribs.
[17] Prasad K, Mullick SC. Heat transfer characteristics of a solar air heater used for drying purposes. Applied Energy 1983;13:8-93.
[18] Gao X, Sundén B. Heat transfer and pressure drop measurements in ribroughened rectangular ducts. Experimental Thermal and Fluid Science 2001;24:25e34.
[19] Han JC, Glicksman LR, Rohsenow WM. An investigation of heat transfer and friction for rib-roughened surfaces. International Journal of Heat and Mass Transfer 1978;21:1143-56.
[20] Prasad BN, Saini JS. Optimal thermohydraulic performance of artificially roughened solar air heaters. Solar Energy 1991;47:91-6.
[21]Taslim ME, Li T, Kercher DM. Darryl E. Metzger memorial session paper:experimental heat transfer and friction in channels roughened with angled, v-shaped,and discrete ribs on two opposite walls. Journal of Turbomachinery 1996;118:20-8.
[22] Webb RL, Eckert ERG, Goldstein RJ. Heat transfer and friction in tubes with repeated-rib roughness. International Journal of Heat and Mass Transfer 1971;14:601-17.
[23] Gao X, Sundén B. Heat transfer distribution in rectangular ducts with v-shaped ribs. Heat and Mass Transfer 2001;37:315-20.
[24] Karwa R. Experimental studies of augmented heat transfer and friction in asymmetrically heated rectangular ducts with ribs on the heated wall in transverse, inclined, v-continuous and v-discrete pattern. International Communications in Heat and Mass Transfer 2003;30:241-50.
[25] Kukreja RT, Lau SC, McMillin RD. Local heat/mass transfer distribution in a square channel with full and v-shaped ribs. International Journal of Heat and Mass Transfer 1993;36:2013-20.
[26] Lau SC, McMillin RD, Han JC. Heat transfer characteristics of turbulent flow in a square channel with angled discrete ribs. Journal of Turbomachinery 1991-113:367e74.
[27] Lanjewar A,Bhagoria JL,Sarviya RM,Heat transfer in solar air heater duct with w-shaped rib roughness on absorber plate.Energy; 2011.doi:10,1016/j.energy.2011.03.054.
[28] Hans VS, Saini RP, Saini JS,Heat transfer and friction factor correlations for a solar air heater duct roughened artificially with multiple v-ribs.Solar Energy 2010;84:898-911.
[29] Bejan A. In: Advanced engineering thermodynamics. New York:Wiley Interscience; 1988. p. 501–14.
[30] Kotas TJ. In: The exergy method of thermal plant analysis. London:Butterworths; 1994. p. 197.
[31] Dincer I, Rosen MA. Exergy as a driver for achieving sustainability.International Journal of Green Energy 2004;1(1):1–19.
[32] Kotas TJ. The exergy method of thermal plant analysis. Malabar,FL: Krieger; 1995 (reprint ed.).
[33] Bejan A. Entropy generation minimization. Boca, Raton, FL: CRC Press; 1996.
[34] Bejan A, Tsatsaronis G,Moran M. Thermal design and optimization. New York: Wiley; 1996.
[35]Wark K. Advanced thermodynamics for engineers. New York:McGraw-Hill; 1995.
[36] Sahu MM, Bhagoria JL. Augmentation of heat transfer coefficient by using 90_broken transverse ribs on absorber plate of solar air heater. Renewable Energy 2005;30(13):2057-73.
[37] Jaurker AR, Saini JS, Gandhi BK. Heat transfer and friction characteristics of rectangular solar air heater duct using rig-grooved artificial roughness. Solar Energy 2006;80(8):895-907.
[38] Karmare SV, Tikekar AN. Heat transfer and friction factor correlation for
[39] Artificially roughened duct with metal grit ribs. Int J Heat Mass Transfer 2007;50(21e22):4342-51.
[40] Layek A, Saini JS, Solanki SC. Heat transfer and friction characteristics for artificially roughened ducts with compound turbulators. Int J Heat Mass Transfer 2007;50(23e24):4845-54.
[41] Aharwal KR, Gandhi BK, Saini JS. Experimental investigation on heat transfer enhancement due to a gap in an inclined continuous rib arrangement in a rectangular duct of solar air heater. Renewable Energy 2008;33(4):585-96.
[42] Varun, Saini RP, Singal SK. Investigation of thermal performance of solar air heater having roughness elements as a combination of inclined and transverse ribs on the absorber plate. Renewable Energy 2008;33(6):1398-405.
[43] Saini RP, Verma J. Heat transfer and friction factor correlations for a duct having dimple shape artificial roughness for solar air heaters. Energy 2008;33(8):1277-87.
[44] Saini SK, Saini RP. Development of correlations for Nusselt number and friction factor for solar air heater with roughened duct having arc shaped wire as artificial roughness. Solar Energy 2008;82(12):1118-30.
[45] Duffie JA, Beckman WA. Solar energy thermal processes. New York: iley and Sons; 1980. p. 211.
[46]Kline SJ, McClintock FA. Describing uncertainties in single sample experiments.J Mech Eng 1953;75:3-8.
[47] Altfeld K, Leiner W, Fiebig M. Second law optimization of flat plate solar air heaters. Part 2: results of optimization and analysis of sensibility to variations of operating conditions. Solar Energy 1988;41(4):309-17.
[48]Kakac S, Shah RK, Aung W. Handbook of single phase convective heat transfer.New York: Wiley; 1987.
[49] Nikuradse J. Law of flow in rough pipes, vol. 1292. National Advisory Committee for Aeronautics Technical Memorandum; 1950.
[50] Gupta D. Investigations on fluid flow and heat transfer in solar air heaters with roughened absorbers. Ph.D. thesis: University of Roorkee. Roorkee (India); 1993.
[51]Webb RL, Eckert ERG, Goldstein RJ. Heat transfer and friction in tubes with repeated rib roughness. Int J Heat Mass Transfer 1971;14(4):601-17.